Research Article

Cyclic Oxygenate-Based Deactivation Mechanism in Dimethyl Ether Carbonylation Reaction over a Pyridine-Modified H-MOR Catalyst

Mingguan Xie, Xudong Fang, Hongchao Liu,* Zhiyang Chen, Bin Li, Leilei Yang, and Wenliang Zhu*
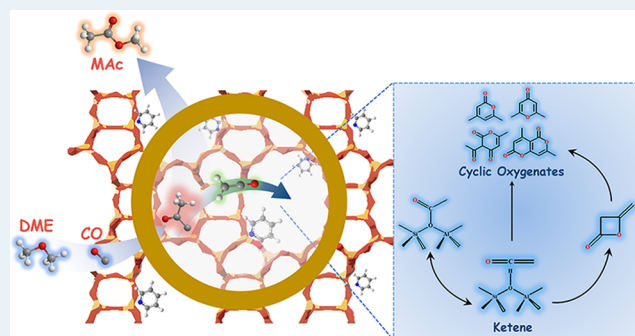
Read Online

ACCESS | Metrics & More | Article Recommendations | Supporting Information

ABSTRACT: The carbonylation of dimethyl ether (DME) over zeolite catalysts breaks through the traditional concept of metal-catalyzed carbonylation and has attracted extensive attention as a critical route for ethanol synthesis. However, the deactivation mechanism during DME carbonylation is complicated and controversial, resulting in great challenges for developing efficient catalysts. Herein, we discovered a catalyst deactivation pathway induced by cyclic oxygenates over the pyridine-modified H-MOR (H-MOR-py) catalyst, which is completely distinct from the classical aromatic-based deactivation route. As the key deactivated species, cyclic oxygenates are generated by the conversion of excessive acetyl groups to ketenes in the eight-membered ring (8-MR) side pockets and further transformation in the 12-MR channel of the H-MOR-py catalyst. A strategy to improve catalyst stability is proposed by rapidly consuming acetyl groups to inhibit the formation of cyclic oxygenates. This study would provide inspiration for DME carbonylation over zeolite catalysts.

KEYWORDS: DME carbonylation, mordenite, deactivation, cyclic oxygenate, acetyl group

■ INTRODUCTION

Ethanol is an important bulk chemical used as an environmentally friendly gasoline additive and raw material for various chemical products.[1,2] Currently, it is mainly produced through the fermentation of starchy crops like corn and wheat.[3] Alternatively, ethanol can be synthesized from syngas (STE) derived from coal, natural gas biomass, and so on.[4] STE via dimethyl ether (DME) carbonylation and the subsequent methyl acetate (MAc) hydrogenation is a promising novel route for ethanol production, owing to its mild reaction conditions, high atomic economy, and friendly environment.[4−6] Since the pioneering works on the acidic zeolites catalyzing methanol and DME carbonylation were reported,[7,8] numerous investigations have been conducted on the design, preparation, and characterization of zeolites catalysts, as well as reaction mechanisms.[8−17] Recently, the role of intermediates during the carbonylation reaction, such as acetyl group, ketene, or acylium ion, has been intensively studied.[18−21] Despite significant progress, achieving high stability of carbonylation catalysts remains a challenging task. Consequently, there is an urgent need to further develop stable catalysts and processes for DME carbonylation, which requires a clear understanding of the deactivation mechanisms involved.

Among the zeolites investigated for the DME carbonylation reaction, H-MOR, which is constituted by an eight-membered ring (8-MR) channel and 12-MR channel with an 8-MR side pocket, is regarded as the optimal catalyst for the DME

carbonylation reaction. Unfortunately, the rapid deactivation poses a great challenge for its potential application as an industrial carbonylation catalyst.[18−20,22−24] It is commonly acknowledged that Brönsted acidic sites (BASs) in the 12-MR channels are primarily responsible for coke formation, leading to rapid deactivation, while BASs in the 8-MR side pocket are active centers for DME carbonylation. Despite extensive research, there are some contradictions regarding the initial precursors of coke formation on H-MOR. DME and MAc are considered to be important sources of coke, which are converted to coke deposition intermediates on the BAS in 12-MR.[22,23] Additionally, ketene, an important intermediate in the DME carbonylation process,[18] is also believed to be involved in coke generation.[19−21] Overall, it is generally accepted that coke formation during the DME carbonylation reaction is analogous to DME or methanol-to-hydrocarbon (DTH/MTH) chemistry, in which olefins/alkyne originating from DME, MAc, or ketenes produce aromatic cokes that result in deactivations.[18−20,22−26] To enhance catalyst stability by avoiding coke formation, many efforts have been
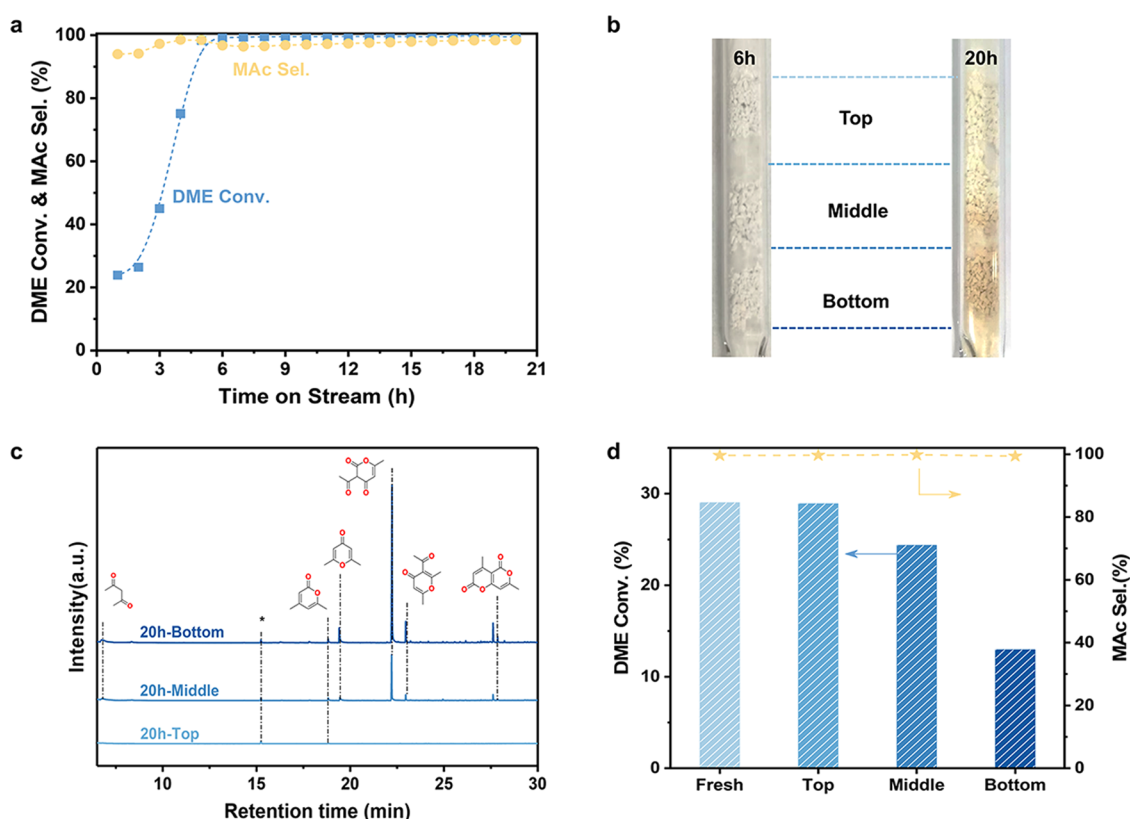
Figure 1. Catalytic and deactivation behavior over H-MOR-py catalyst for DME carbonylation. (a) DME conversion and MAc selectivity of H-MOR-py with time on stream. (b) Photographs of catalysts after reactions for different times. (c) GC-MS analyses for retained species in different catalyst beds after the reaction. The internal standard peak C_2Cl_6 (10 ppm) was indicated by * in the chromatograms, the same in this paper. (d) DME conversion and MAc selectivity of fresh H-MOR-py and spent H-MOR-py in different catalyst beds after the reaction 20 h of (a); the rate at TOS 20 h is in a steady state. Reaction conditions: (a−c) 463 K, 2 MPa, gas hourly space velocity (GHSV) = 2000 h^{-1}, $n_{DME}/n_{CO}/n_{H_2}$ = 5/35/60. (d) 463 K, 2 MPa, GHSV = 15,000 h^{-1}, TOS = 20 h, $n_{DME}/n_{CO}/n_{H_2}$ = 5/35/60.

implemented to eliminate or shield the acid sites in 12-MR using steam treatment, alkaline/acid media treatment, or selective adsorption pyridine.[27−30] The stability of pyridine-modified H-MOR (H-MOR-py) is improved obviously as pyridine can selectively enter and completely shield the acid sites in 12-MR channels of H-MOR. However, gradual deactivation can still be observed on H-MOR-py during DME carbonylation.[29−31] This prompts us to consider whether there is a deactivation pathway caused only by acid sites in 8-MR of H-MOR during the reaction.

Herein, we investigate the evolution of deposited species in the H-MOR-py catalyst during the DME carbonylation reaction. For the first time, abundant cyclic oxygenates are detected on the H-MOR-py catalyst and proven to result in catalyst deactivation, which differs from the general cognition of the deactivation caused by the aromatic hydrocarbons originating from the DTH/MTH reaction. According to various characterizations and probe experiments, we outline a unique formation roadmap of cyclic oxygenated species during the DME carbonylation reaction. Furthermore, an effective strategy is proposed to inhibit coke formation based on an understanding of the deactivation mechanism.

■ RESULTS AND DISCUSSION

Unique Deactivation Behavior of H-MOR-py in DME Carbonylation. The detailed structural properties and chemical information on the catalysts are shown in Figure S1

and Table S1. Remarkably, FT-IR spectra in Figure S1d shows the hydroxyl vibration region of H-MOR-py catalyst only observed at 3590 cm^{-1}, indicating that BAS only in the 8-MR side pockets and the acid sites in 12-MR of the catalyst has been completely shielded.[10,31−33] H-MOR-py catalysts were loaded in a continuous flow fixed-bed stainless steel reactor equipped with a quartz lining and divided into three layers by quartz wool. DME carbonylation performance at 463 K, 2 MPa, and 2000 h^{-1} is shown in Figures 1a and S2, along with images of spent catalysts after different times in Figure 1b. After an induction period of 6 h, nearly 100% DME conversion can be achieved (Figure 1a), and the color of the spent catalyst is almost identical across all layers at that time (Figure 1b). Surprisingly, as the reaction proceeds to 20 h, the color of the spent catalyst darkens from the top to the bottom layers (Figure 1b). Furthermore, TG analysis indicates that the largest amount of deposition species is found in the spent catalysts collected from the bottom layer (Figure S3 and Table S2). These observations are distinct from those in traditional DTH/MTH reactions, in which the color of the spent catalyst in the top layer is the darkest in the whole reactor and the reaction zone gradually migrates downward with the reaction proceeding.[25,26,34,35]

The retained species in the spent H-MOR-py were identified using Guisnet's method.[36] Figures 1c and S4 illustrate the identifications for the retained species and their evolution with time on stream (TOS) and loading positions. After 6 h of reaction, trace cyclic oxygenated compounds, including 4,6-
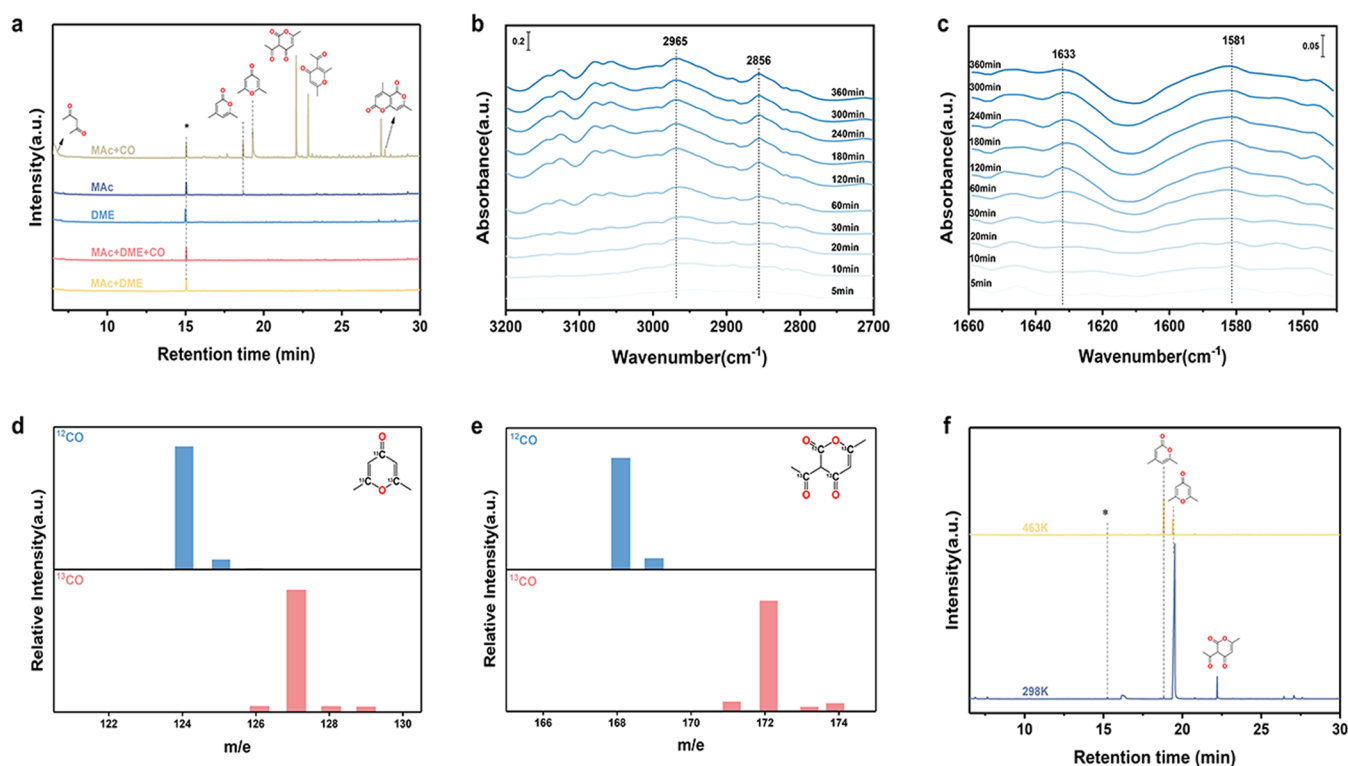
Figure 2. Characterization to prove the formation way of cyclic oxygenates retained in the H-MOR-py catalyst. (a) GC-MS analyses for retained species in the spent catalyst after the reaction with different reactants. (b, c) In situ diffuse reflectance Fourier transform (DRIFT) spectra of H-MOR-py during the DME carbonylation reaction. (d, e) MS spectra of 2,6-dimethyl-4-pyrone (d) and dehydroacetic acid (e) in ^{12}CO (top) and ^{13}CO (bottom) during the DME carbonylation reaction. (f) GC-MS analyses for retained species in the spent catalyst after the reaction with acetyl ketene as a probe molecule at different reaction temperatures. Reaction conditions: (a) 463 K, 2 MPa, GHSV = 24,000 h^{-1}, Ar as balance gas. MAc + CO: 12.3 kPa MAc, 172.8 kPa CO; MAc + DME + CO: 12.3 kPa MAc, 6.2 kPa DME, 172.8 kPa CO; MAc: 12.3 kPa MAc; MAc + DME: 6.2 kPa DME, 12.3 kPa MAc; DME: 6.2 kPa DME; DME + CO: 6.2 kPa DME, 172.8 kPa CO. (b, c) 473 K, 1 MPa, and $n_{DME}/n_{CO} = 1/49$. (d, e) 473 K, 0.5 MPa, $n_{DME}/n_{CO} = 1/80$, GHSV = 1200 h^{-1}. (f) 2 MPa, GHSV = 24,000 h^{-1}, Ar as balance gas.

dimethyl-2-pyrone and dehydroacetic acid, are captured in the spent catalysts of the down layer, while these compounds are hardly detected in the spent catalysts of the top and middle layers (Figure S4). With the reaction proceeding for 20 h, evident differences in the amount of retained species are observed with the loading positions (Figure 1c). Specifically, abundant cyclic oxygenated compounds, such as 4,6-dimethyl-2-pyrone, 2,6-dimethyl-4-pyrone, dehydroacetic acid, 4,7-dimethyl-2*H*,5*H*-pyrano[4,3-*b*] pyran-2,5-dione, etc., are found to be retained in the bottom-layer catalysts. Moreover, the content of oxygenates in the middle and bottom catalysts is much greater than those in the top catalysts, consistent with the TG results.

Polycyclic aromatic hydrocarbons (PAHs), the deactivation species in DTH/MTH reactions,[25,26,34,35] have been regarded to be responsible for the deactivation of H-MOR (with acid sites in both 8-MR side pocket and 12-MR channel) during DME carbonylation.[18−20,22−24] However, PAHs are hardly detected in the H-MOR-py catalyst (with only acid sites in the 8-MR side pocket) in our study. To clarify the influence of the oxygenates on the catalytic performance of the DME carbonylation reaction, the spent samples at TOS of 20 h in different layers and the fresh sample were evaluated at 463 K, 2 MPa, and 15,000 h^{-1}. As shown in Figure 1d, the DME conversion (∼29%) of the spent samples in the top layer is almost the same as that of the fresh sample. However, an obvious decrease in DME conversion can be observed in the spent catalysts of the middle and bottom layers (∼25 and

∼13%, respectively). Combined with the retained species distribution in different layers, we can confirm that the cyclic oxygenate deposited in H-MOR-py is one of the important factors leading to the deactivation of the DME carbonylation. Therefore, we speculate that there should be a unique deactivation mechanism based on cyclic oxygenate during the DME carbonylation reaction over the H-MOR-py catalyst.

Formation Route of Cyclic Oxygenate in H-MOR-py. To identify the origin of the cyclic oxygenates, DME, MAc, or their mixture is employed as reactants on H-MOR-py under a CO-free or a CO atmosphere at 463 K and 2 MPa for 6 h (Figures 2a and S5). The focus is mainly on the differences in the species deposited in H-MOR-py. Obvious distinctions can be observed when DME or MAc is used as a reactant. A trace amount of cyclic oxygenates, such as 4,6-dimethyl-2-pyrone, is detected on the catalyst when MAc is used as a reactant, while nothing is found when DME is employed. Notably, a larger amount of cyclic oxygenated species is captured in H-MOR-py when co-feeding MAc and CO into the reaction system, which is consistent with those in Figure 1c. These suggest that the formation of cyclic oxygenates in H-MOR-py might be related to MAc or its induced intermediate species, and the presence of CO accelerates their generation. Interestingly, cyclic oxygenates cannot be detected when co-feeding the mixtures of MAc and DME under the CO-free or CO atmosphere with the constant MAc partial pressure, indicating that the presence of DME inhibits the formation of oxygenated compounds. Under a CO atmosphere, MAc can produce acetyl groups
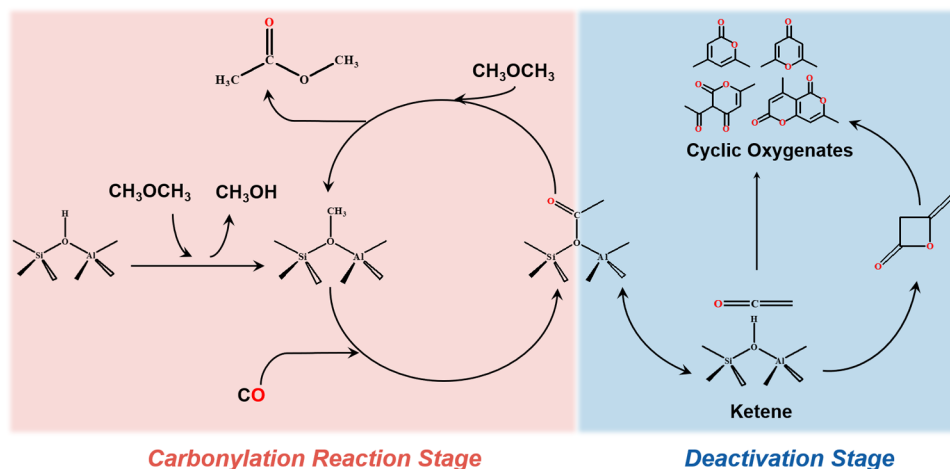
Figure 3. Cyclic oxygenate-based deactivation mechanism proposed for DME carbonylation.

through direct adsorption or the carbonylation reaction of its methyl group on H-MOR-py catalysts.[37] Consequently, the environment of excessive acetyl groups should exist when co-feeding MAc and CO. Thus, we deduce that the formation of cyclic oxygenates might be related to the excessive acetyl groups, which are retained in the H-MOR-py catalyst due to the failure to react with the methoxy group of DME in time to form a more stable MAc.

In order to further verify the role of the acetyl groups in the formation of cyclic oxygenates, more experiments were conducted such as in situ DRIFT experiments and ^{13}C isotope tracing. As shown in Figure 2b,2c, the evolution of the surface species over the H-MOR-py is monitored at different reaction times using in situ DRIFT. The bands at 2965 and 2865 cm^{-1}, attributed to the surface methoxy group,[19,22] appear when DME and CO are introduced into the reaction system. The relative intensities increase initially with reaction times and remain constant after 2 h, indicating that DME is absorbed initially and reaches a dynamic equilibrium between the adsorption and reaction of DME on BAS in 8-MR of H-MOR-py after 2 h. The band at 1633 cm^{-1} assigned to acetyl groups[19,20] appears along with increases of the peak attributed methoxy group, reaching a maximum at 2 h and then decreasing. A new band at 1581 cm^{-1}, assigned to the vibration of cyclic oxygenates (Figure S6), appears and increases, accompanied by a decrease in the peak attributed to the acetyl group. These observations suggest that the carbonylation reaction occurs and cyclic oxygenates in the H-MOR-py are produced from acetyl groups.

Furthermore, a ^{13}C isotope tracing experiment was carried out to verify our speculation. After DME was fed with ^{12}CO or ^{13}CO, massive cyclic oxygenates were both found on the H-MOR-py catalyst. Specifically, feeding ^{13}CO as a reactant shifts the mass pattern to larger masses (Figures 2d,e and S7). The resulting mass increment of each maximum peak relative to that for ^{12}CO as the reactant corresponds to the exact number of CO insertions (denoted as $n(\mathrm{CO})$). Mathematically, the value is half the number of carbon atoms in the corresponding oxygenates with an even carbon number (denoted as $n(\mathrm{e})$, $n(\mathrm{e}) = 2 \times n(\mathrm{CO})$), indicating that half of the carbon in the formation of oxygenates comes from CO, in line with the polymerization of acetyl groups. As for oxygenates with an odd carbon number (denoted as $n(\mathrm{o})$), the addition of one carbon number is twice the addition of one CO insertion number

($n(\mathrm{o}) + 1 = 2 \times (n(\mathrm{CO}) + 1)$), suggesting that there should be a decarbonylation or a methylation during the reaction apart from the polymerization of acetyl groups. ^{13}C MAS NMR spectra of the solutions display signals at 201.4, 190.4, 179.1, 164.8, and 148.6 ppm (Figure S8), attributed to the C atoms in the cyclic oxygenates. These results confirm that CO is inserted into the oxygenated species. Consequently, it can be concluded that the formation of cyclic oxygenates is directly related to the acetyl groups.

To further validate whether the acetyl group can be converted into oxygenates, probe experiments were carried out. As shown in Figure S9, a substantial number of cyclic oxygenated compounds, such as 4,6-dimethyl-2-pyrone, 2,6-dimethyl-4-pyrone, dehydroacetic acid, etc., are found when acetic anhydride (Ac$_2$O) is introduced into the H-MOR-py catalyst at 463 K and 2 MPa. Moreover, these oxygenates are also detected in the spent catalyst when co-feeding CH$_3$Cl and CO at 463 K and 2 MPa. It is known that Ac$_2$O[38] and the carbonylation of CH$_3$Cl[39] can produce acetyl groups on the zeolite catalyst. Thus, it is convincing that cyclic oxygenates can be produced by the acetyl groups. In addition, there is no methyl group during the Ac$_2$O probe experiment, indicating that cyclic oxygenates should be formed by the polymerization and decarbonylation of acetyl groups.

The acetyl group is suggested to be relatively stable within the confined 8-MR side pocket due to its interaction with the H-MOR framework.[18,20,40] Moreover, it is almost impossible for the small 8-MR side pocket of the H-MOR-py catalyst to provide enough space to accommodate such bulky cyclic oxygenates due to steric hindrance. These inspired us to consider how acetyl groups are converted to cyclic oxygenates. Notably, the acetyl group has been identified as a derivative of highly reactive ketene, which is supposed to be an important intermediate to form MAc.[20,21] More importantly, the ketene is also detrimental to DME carbonylation as it results in catalyst deactivation, which can be transformed into aromatics cokes via olefins or acetyl ketene-diene/alkyne.[18−20,40] Interestingly, massive cyclic oxygenates instead of aromatic cokes are found in our experiments. These observations indicate that a new ketene conversion pathway should exist in H-MOR-py catalysts without acid sites in the 12-MR channel. In addition, ketene is readily dimerized to acetyl ketene in the zeolite as a thermodynamically favorable process.[20,37,41] Therefore, we used acetyl ketene as a probe molecule in the H-MOR-py
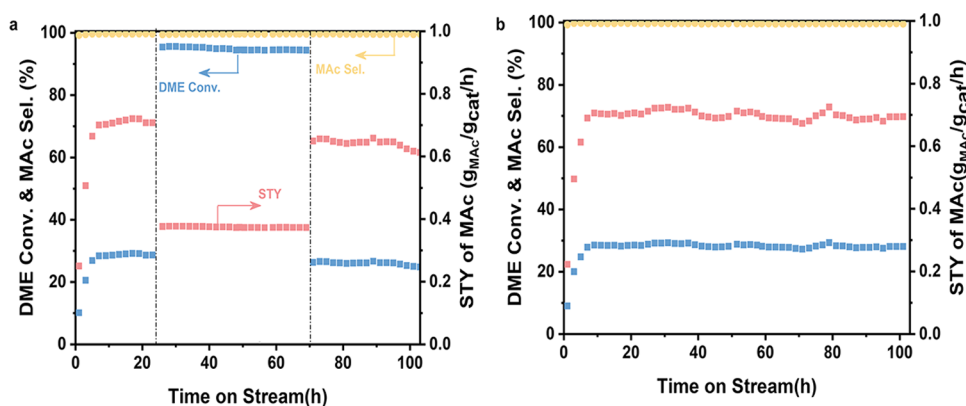
Figure 4. Stability test for the DME carbonylation over the H-MOR-py catalyst. Reaction conditions: 463 K, 2 MPa. $n_{DME}/n_{CO}/n_{H_2}$ = 5/35/60. (a) GHSV = 15,000 h^{-1} at TOS 0−23 h, GHSV = 2400 h^{-1} at TOS 24−70 h, GHSV = 15,000 h^{-1} at TOS 71−100 h. (b) GHSV = 15,000 h^{-1} for 100 h.

catalyst to study the ketene conversion. As shown in Figure 2f, oxygenates such as dehydroacetic acid and 2,6-dimethyl-4-pyrone are found in the catalyst at 298 K. After increasing the temperature to 463 K, dehydroacetic acid disappears along with the amount of 4,6-dimethyl-2-pyrone increases. The phenomenon is consistent with previous studies that dehydroacetic acid can be dimerized from acetyl ketene; 2,6-dimethyl-4-pyrone can be dimerized from acetyl ketene and further decarboxylated.[37,41,42] Overall, these results indicate that oxygenates can be formed by the successive polymerization and decarbonylation reaction of ketenes.

The N$_2$ physical adsorption and desorption results show that the micropore area and volume of the spent catalyst (the deactivated catalyst in the bottom layer of Figure 1a) decrease significantly from the initial 197 to 35 m^2/g and 0.092 to 0.016 cm^3/g, respectively (Table S1). These results indicate that the oxygenated species might be located in the 12-MR channel of H-MOR-py due to the highly steric hindrance in the 8-MR side pocket. To clarify the role of the 12-MR channel in forming oxygenates, we introduced acetyl ketene into Na-MOR without BAS and H-MOR with BAS at 463 K and 2 MPa, respectively. As shown in Figure S10, the oxygenates are detected in the Na-MOR, suggesting that the 12-MR pore without BAS provides a confined space for oxygenate formation. Interestingly, in addition to cyclic oxygenates, additional aromatic species are observed on H-MOR (Figure S11), which is consistent with previous studies,[19,20] suggesting that BAS in 12-MR of H-MOR catalyst can alter the conversion pathways of ketene/acetyl ketene. In all, it can be deduced that the BAS in 8-MR favors the formation of highly reactive ketene, and the 12-MR channel provides sufficient accommodation for the successive conversion of ketene into bulky cyclic oxygenates for the H-MOR-py catalyst.

Based on the results presented above, we have outlined a unique deactivation route map for the DME carbonylation in H-MOR-py, as shown in Figure 3. Typically, DME and hydrogen protons in the zeolite react to form surface methoxy groups. Subsequently, the carbonylation reaction of surface methoxy groups and CO leads to the formation of acetyl groups, which then react with the methoxy of DME to produce MAc. More importantly, there exists a dynamic equilibrium between the acetyl group and ketene, and the equilibrium tends to shift to ketene if the acetyl group fails to react with DME in time. Finally, ketene or acetyl ketene triggers the

generation of cyclic oxygenated compounds by polymerization and decarbonylation, including 4,6-dimethyl-2-pyrone, 2,6-dimethyl-4-pyrone, dehydroacetic acid, 4,7-dimethyl-2*H*,5*H*-pyrano[4,3-*b*] pyran-2,5-dione, etc., which are detrimental to the catalyst activity during the reaction.

Strategy to Prevent Coke Formation. On the basis of the understanding of the deactivation mechanism, we designed stability tests via controlling the content of acetyl groups by adjusting DME conversion during the reaction to clarify their effect on the catalyst stability. As shown in Figure 4a, the reaction is initially carried out with ∼28 to ∼29% DME conversion and 0.70 g g$_{cat.}^{-1}$ h^{-1} MAc space-time yield (STY) after an introduction period at 463 K and 2 MPa with a GHSV of 15,000 h^{-1}. When GHSV is decreased to 2400 h^{-1} at TOS 24−70 h, the DME conversion is increased to ∼94−95%. After GHSV is increased back to 15,000 h^{-1}, the MAc STY decreases from the initial 0.70 g g$_{cat.}^{-1}$ h^{-1} to 0.65 g g$_{cat.}^{-1}$ h^{-1}. Additionally, compared to the initial stage (TOS 0−23 h), the stability becomes poor and MAc STY continues to decrease to 0.60 g g$_{cat.}^{-1}$ h^{-1} at TOS 100 h. The decline in catalyst stability may be attributed to a large amount of acetyl groups that are not consumed in time at such a high DME conversion at TOS 24 h−70 h, resulting in more acetyl groups being retained in the catalyst and generating more cyclic oxygenates. Interestingly, when GHSV was maintained at 15,000 h^{-1} throughout the reaction, the catalytic activity remained stable within 100 h with ∼28 to ∼29% DME conversion and ∼0.70 g g$_{cat.}^{-1}$ h^{-1} MAc STY (Figure 4b). In contrast, when GHSV was maintained at 2400 h^{-1}, the DME conversion can reach up to ∼95% after the induction period but decreases to ∼89% within 100 h (Figure S12). These indicate that DME with a high concentration in the reaction system plays an important role in enhancing stability by consuming acetyl groups quickly. Moreover, the GC-MS analysis of the spent catalysts after two tests in Figure 4 revealed that the H-MOR-py catalyst in Figure 4b had fewer remaining carbon deposits (Figure S13), although it produced more MAc, indicating that consuming acetyl groups quickly during the reaction can reduce oxygenated coke formation.

Furthermore, we investigated the influence of the reaction temperature on stability. As shown in Figure S14, the stability is poorer at higher temperatures (503 K) compared to that at the lower reaction temperature (463 K) in Figure 4. Correspondingly, many more cyclic oxygenates can be

captured for the spent catalyst evaluated at 503 K. These prove further that minimizing the accumulation and reaction of excess acetyl groups will be beneficial for improving the stability of the DME carbonylation reaction. Accordingly, there should be many other strategies such as modifying the reaction conditions or catalyst design to optimize the stability based on our proposed deactivation mechanism.

CONCLUSIONS

In summary, we have successfully demonstrated a unique deactivation roadmap induced by cyclic oxygenates for DME carbonylation over H-MOR-py zeolites through various characterizations and probe experiments. Abundant cyclic oxygenated compounds retained in the H-MOR-py catalyst are first reported to be detrimental to the catalyst activity during the DME carbonylation reaction. It has been demonstrated that the excessive acetyl group on the BAS in the H-MOR-py 8-MR side pocket, which is retained in the catalyst due to the failure to react with the methoxy group of DME in time to form a more stable MAc, tends to form ketenes in 8-MR and their successive conversion to produce cyclic oxygenates by the reaction of polymerization and decarbonylation in 12-MR channel without the BAS. Based on this understanding, the strategy of consuming and minimizing excessive acetyl groups during the reaction is proposed and verified to achieve excellent catalyst stability. It is expected that the deactivation mechanism proposed in this work will guide rational catalyst design for the DME carbonylation reaction and provide theoretical guidance for industrial production.

ASSOCIATED CONTENT

ⓈI Supporting Information

The Supporting Information is available free of charge at https://pubs.acs.org/doi/10.1021/acscatal.3c04344.

> Complete experimental procedures, supplementary characterization data, and supplementary experimental data (PDF)

AUTHOR INFORMATION

Corresponding Authors

Hongchao Liu − *National Engineering Research Center of Lower-Carbon Catalysis Technology, Dalian Institute of Chemical Physics, Chinese Academy of Sciences, Dalian 116023 Liaoning, China*; Email: chliu@dicp.ac.cn

Wenliang Zhu − *National Engineering Research Center of Lower-Carbon Catalysis Technology, Dalian Institute of Chemical Physics, Chinese Academy of Sciences, Dalian 116023 Liaoning, China;* ⓞ orcid.org/0000-0002-2247-6849; Email: wlzhu@dicp.ac.cn

Authors

Mingguan Xie − *National Engineering Research Center of Lower-Carbon Catalysis Technology, Dalian Institute of Chemical Physics, Chinese Academy of Sciences, Dalian 116023 Liaoning, China; University of Chinese Academy of Sciences, Beijing 100049, China*

Xudong Fang − *National Engineering Research Center of Lower-Carbon Catalysis Technology, Dalian Institute of Chemical Physics, Chinese Academy of Sciences, Dalian 116023 Liaoning, China; University of Chinese Academy of Sciences, Beijing 100049, China*

Zhiyang Chen − *National Engineering Research Center of Lower-Carbon Catalysis Technology, Dalian Institute of Chemical Physics, Chinese Academy of Sciences, Dalian 116023 Liaoning, China*

Bin Li − *National Engineering Research Center of Lower-Carbon Catalysis Technology, Dalian Institute of Chemical Physics, Chinese Academy of Sciences, Dalian 116023 Liaoning, China; University of Chinese Academy of Sciences, Beijing 100049, China*

Leilei Yang − *National Engineering Research Center of Lower-Carbon Catalysis Technology, Dalian Institute of Chemical Physics, Chinese Academy of Sciences, Dalian 116023 Liaoning, China; University of Chinese Academy of Sciences, Beijing 100049, China*

Complete contact information is available at:
https://pubs.acs.org/10.1021/acscatal.3c04344

Notes

The authors declare no competing financial interest.

ACKNOWLEDGMENTS

REFERENCES

(1) Farrell, A. E.; Plevin, R. J.; Turner, B. T.; Jones, A. D.; O'Hare, M.; Kammen, D. M. Ethanol Can Contribute to Energy and Environmental Goals. *Science* **2006**, *311* (5760), 506−508.

(2) Ni, M.; Leung, D. Y. C.; Leung, M. K. H. A review on reforming bio-ethanol for hydrogen production. *Int. J. Hydrogen Energy* **2007**, *32* (15), 3238−3247.

(3) Bušić, A.; Marđetko, N.; Kundas, S.; Morzak, G.; Belskaya, H.; Ivančić Šantek, M.; Komes, D.; Novak, S.; Šantek, B. Bioethanol Production from Renewable Raw Materials and Its Separation and Purification: A Review. *Food Technol. Biotechnol.* **2018**, *56* (3), 289−311.

(4) Liu, G.; Yang, G.; Peng, X.; Wu, J.; Tsubaki, N. Recent advances in the routes and catalysts for ethanol synthesis from syngas. *Chem. Soc. Rev.* **2022**, *51* (13), 5606−5659.

(5) Lu, P.; Chen, Q.; Yang, G.; Tan, L.; Feng, X.; Yao, J.; Yoneyama, Y.; Tsubaki, N. Space-Confined Self-Regulation Mechanism from a Capsule Catalyst to Realize an Ethanol Direct Synthesis Strategy. *ACS Catal.* **2020**, *10* (2), 1366−1374.

(6) Zhang, F.; Chen, Z.; Fang, X.; Liu, H.; Liu, Y.; Zhu, W. Catalytic activity of Cu/ZnO catalysts mediated by MgO promoter in hydrogenation of methyl acetate to ethanol. *J. Energy Chem.* **2021**, *61*, 203−209.

(7) Fujimoto, K.; Shikada, T.; Omata, K.; Tominaga, H.-o. Vapor phase carbonylation of methanol with solid acid catalysts. *Chem. Lett.* **1984**, *13* (12), 2047−2050.

(8) Cheung, P.; Bhan, A.; Sunley, G. J.; Iglesia, E. Selective Carbonylation of Dimethyl Ether to Methyl Acetate Catalyzed by Acidic Zeolites. *Angew. Chem., Int. Ed.* **2006**, *45* (10), 1617−1620.

(9) Cheung, P.; Bhan, A.; Sunley, G. J.; Law, D. J.; Iglesia, E. Site requirements and elementary steps in dimethyl ether carbonylation catalyzed by acidic zeolites. *J. Catal.* **2007**, *245* (1), 110−123.

(10) Bhan, A.; Allian, A. D.; Sunley, G. J.; Law, D. J.; Iglesia, E. Specificity of Sites within Eight-Membered Ring Zeolite Channels for Carbonylation of Methyls to Acetyls. *J. Am. Chem. Soc.* **2007**, *129* (16), 4919−4924.

(11) Chu, W.; Liu, X.; Yang, Z.; Nakata, H.; Tan, X.; Liu, X.; Xu, L.; Guo, P.; Li, X.; Zhu, X. Constrained Al sites in FER-type zeolites. *Chin. J. Catal.* **2021**, *42* (11), 2078−2087.

(12) Feng, X.; Yao, J.; Li, H.; Fang, Y.; Yoneyama, Y.; Yang, G.; Tsubaki, N. A brand new zeolite catalyst for carbonylation reaction. *Chem. Commun.* **2019**, *55* (8), 1048−1051.

(13) Xiong, Z.; Zhan, E.; Li, M.; Shen, W. DME carbonylation over a HSUZ-4 zeolite. *Chem. Commun.* **2020**, *56* (23), 3401−3404.

(14) Park, S. Y.; Shin, C.-H.; Bae, J. W. Selective carbonylation of dimethyl ether to methyl acetate on Ferrierite. *Catal. Commun.* **2016**, *75*, 28−31.

(15) Lusardi, M.; Chen, T. T.; Kale, M.; Kang, J. H.; Neurock, M.; Davis, M. E. Carbonylation of Dimethyl Ether to Methyl Acetate over SSZ-13. *ACS Catal.* **2020**, *10* (1), 842−851.

(16) Boronat, M.; Martínez-Sánchez, C.; Law, D.; Corma, A. Enzyme-like Specificity in Zeolites: A Unique Site Position in Mordenite for Selective Carbonylation of Methanol and Dimethyl Ether with CO. *J. Am. Chem. Soc.* **2008**, *130* (48), 16316−16323.

(17) Xiong, Z.; Qi, G.; Zhan, E.; Chu, Y.; Xu, J.; Wei, J.; Ta, N.; Hao, A.; Zhou, Y.; Deng, F.; Shen, W. Experimental identification of the active sites over a plate-like mordenite for the carbonylation of dimethyl ether. *Chem* **2023**, *9* (1), 76−92.

(18) Rasmussen, D. B.; Christensen, J. M.; Temel, B.; Studt, F.; Moses, P. G.; Rossmeisl, J.; Riisager, A.; Jensen, A. D. Ketene as a Reaction Intermediate in the Carbonylation of Dimethyl Ether to Methyl Acetate over Mordenite. *Angew. Chem., Int. Ed.* **2015**, *54* (25), 7261−7264.

(19) Cheng, Z.; Huang, S.; Li, Y.; Cai, K.; Wang, Y.; Wang, M.-y.; Lv, J.; Ma, X. Role of Brønsted Acid Sites within 8-MR of Mordenite in the Deactivation Roadmap for Dimethyl Ether Carbonylation. *ACS Catal.* **2021**, *11* (9), 5647−5657.

(20) Chen, W.; Li, G.; Yi, X.; Day, S. J.; Tarach, K. A.; Liu, Z.; Liu, S.-B.; Edman Tsang, S. C.; Góra-Marek, K.; Zheng, A. Molecular Understanding of the Catalytic Consequence of Ketene Intermediates under Confinement. *J. Am. Chem. Soc.* **2021**, *143* (37), 15440−15452.

(21) Chen, W.; Tarach, K. A.; Yi, X.; Liu, Z.; Tang, X.; Góra-Marek, K.; Zheng, A. Charge-separation driven mechanism via acylium ion intermediate migration during catalytic carbonylation in mordenite zeolite. *Nat. Commun.* **2022**, *13* (1), No. 7106.

(22) Zhou, H.; Zhu, W.; Shi, L.; Liu, H.; Liu, S.; Ni, Y.; Liu, Y.; He, Y.; Xu, S.; Li, L.; Liu, Z. In situ DRIFT study of dimethyl ether carbonylation to methyl acetate on H-mordenite. *J. Mol. Catal. A: Chem.* **2016**, *417*, 1−9.

(23) Wang, X.; Li, R.; Yu, C.; Liu, Y.; Xu, C.; Lu, C. Study on the deactivation process of dimethyl ether carbonylation reaction over Mordenite catalyst. *Fuel* **2021**, *286*, No. 119480.

(24) Li, B.; Xu, J.; Han, B.; Wang, X.; Qi, G.; Zhang, Z.; Wang, C.; Deng, F. Insight into Dimethyl Ether Carbonylation Reaction over Mordenite Zeolite from in-Situ Solid-State NMR Spectroscopy. *J. Phys. Chem. C* **2013**, *117* (11), 5840−5847.

(25) Tian, P.; Wei, Y.; Ye, M.; Liu, Z. Methanol to Olefins (MTO): From Fundamentals to Commercialization. *ACS Catal.* **2015**, *5* (3), 1922−1938.

(26) Lin, S.; Zhi, Y.; Chen, W.; Li, H.; Zhang, W.; Lou, C.; Wu, X.; Zeng, S.; Xu, S.; Xiao, J.; Zheng, A.; Wei, Y.; Liu, Z. Molecular Routes of Dynamic Autocatalysis for Methanol-to-Hydrocarbons Reaction. *J. Am. Chem. Soc.* **2021**, *143* (31), 12038−12052.

(27) Xue, H.; Huang, X.; Zhan, E.; Ma, M.; Shen, W. Selective dealumination of mordenite for enhancing its stability in dimethyl ether carbonylation. *Catal. Commun.* **2013**, *37*, 75−79.

(28) Liu, R.; Fan, B.; Zhang, W.; Wang, L.; Qi, L.; Wang, Y.; Xu, S.; Yu, Z.; Wei, Y.; Liu, Z. Increasing the Number of Aluminum Atoms in T3 Sites of a Mordenite Zeolite by Low-Pressure SiCl$_4$ Treatment to Catalyze Dimethyl Ether Carbonylation. *Angew. Chem., Int. Ed.* **2022**, *61* (18), No. e202116990.

(29) Liu, J.; Xue, H.; Huang, X.; Wu, P.-H.; Huang, S.-J.; Liu, S.-B.; Shen, W. Stability Enhancement of H-Mordenite in Dimethyl Ether Carbonylation to Methyl Acetate by Pre-adsorption of Pyridine. *Chin. J. Catal.* **2010**, *31* (7), 729−738.

(30) Liu, R.; Fan, B.; Zhi, Y.; Liu, C.; Xu, S.; Yu, Z.; Liu, Z. Dynamic Evolution of Aluminum Coordination Environments in Mordenite Zeolite and Their Role in the Dimethyl Ether (DME) Carbonylation Reaction. *Angew. Chem., Int. Ed.* **2022**, *61* (42), No. e202210658.

(31) Cao, K.; Fan, D.; Li, L.; Fan, B.; Wang, L.; Zhu, D.; Wang, Q.; Tian, P.; Liu, Z. Insights into the Pyridine-Modified MOR Zeolite Catalysts for DME Carbonylation. *ACS Catal.* **2020**, *10* (5), 3372−3380.

(32) Zholobenko, V. L.; Makarova, M. A.; Dwyer, J. Inhomogeneity of Bronsted acid sites in H-mordenite. *J. Phys. Chem. C* **1993**, *97* (22), 5962−5964.

(33) Wakabayashi, F.; Kondo, J.; Wada, A.; Domen, K.; Hirose, C. FT-IR Studies of the Interaction Between Zeolitic Hydroxyl-groups and Small Molecules. 1. Adsorption of Nitrogen on H-mordenite at Low-temperature. *J. Phys. Chem. A* **1993**, *97* (41), 10761−10768.

(34) Wang, N.; Zhi, Y.; Wei, Y.; Zhang, W.; Liu, Z.; Huang, J.; Sun, T.; Xu, S.; Lin, S.; He, Y.; Zheng, A.; Liu, Z. Molecular elucidating of an unusual growth mechanism for polycyclic aromatic hydrocarbons in confined space. *Nat. Commun.* **2020**, *11* (1), No. 1079.

(35) Kaarsholm, M.; Joensen, F.; Nerlov, J.; Cenni, R.; Chaouki, J.; Patience, G. S. Phosphorous modified ZSM-5: Deactivation and product distribution for MTO. *Chem. Eng. Sci.* **2007**, *62* (18), 5527−5532.

(36) Guisnet, M.; Magnoux, P. Coking and deactivation of zeolites − influence of the pore structure. *Appl. Catal.* **1989**, *54* (1), 1−27.

(37) Zhou, Z.; Liu, H.; Ni, Y.; Wen, F.; Chen, Z.; Zhu, W.; Liu, Z. Direct conversion of dimethyl ether and CO to acetone via coupling carbonylation and ketonization. *J. Catal.* **2021**, *396*, 360−373.

(38) Chen, Z.; Ni, Y.; Zhi, Y.; Wen, F.; Zhou, Z.; Wei, Y.; Zhu, W.; Liu, Z. Coupling of Methanol and Carbon Monoxide over H-ZSM-5 to Form Aromatics. *Angew. Chem., Int. Ed.* **2018**, *57* (38), 12549−12553.

(39) Fang, X.; Wen, F.; Ding, X.; Liu, H.; Chen, Z.; Liu, Z.; Liu, H.; Zhu, W.; Liu, Z. Highly Selective Carbonylation of CH$_3$Cl to Acetic Acid Catalyzed by Pyridine-Treated MOR Zeolite. *Angew. Chem., Int. Ed.* **2022**, *61* (31), No. e202203859.

(40) Chowdhury, A. D.; Gascon, J. The Curious Case of Ketene in Zeolite Chemistry and Catalysis. *Angew. Chem., Int. Ed.* **2018**, *57* (36), 14982−14985.

(41) Hassanpour, J.; Zamani, M.; Dabbagh, H. A. Effect of ketene additive and Si/Al ratio on the reaction of methanol over HZSM-5 catalysts. *Appl. Organomet. Chem.* **2018**, *32* (3), No. e4133.

(42) Clemens, R. J. Diketene. *Chem. Rev.* **1986**, *86* (2), 241−318.